minerals

MDPI

Article

Determination of Abrasiveness in Copper-Gold Sulfide Ores: A Contribution to the Geometallurgical Model of the Sossego Deposit

Petterson de Azevedo Barbosa [1,*], Maurício Guimarães Bergerman [1,*], Elisabeth da Fonseca [2] and Rogerio Kwitko-Ribeiro [2]

[1] Department of Mining and Petroleum Engineering, Polytechnical School, University of São Paulo, São Paulo 05508-030, SP, Brazil
[2] Mineral Development Center, Vale S.A., Santa Luzia 33040-900, MG, Brazil; elisabeth.fonseca@vale.com (E.d.F.); rogerio.kwitko@vale.com (R.K.-R.)
* Correspondence: petterson.barbosa@usp.br (P.d.A.B.); mbergerman@usp.br (M.G.B.)

Abstract: The geological context of this study is established in the iron oxide-copper-gold (IOCG) deposit of Sossego (Canaã dos Carajás, Brazil), where hydrothermal alterations in shear zones concentrated the metals of interest and added new characteristics to the metavolcanic-sedimentary and granite rocks. The mineral transformation of rocks by hypersaline fluids enriched in metals and silica also modifies some metallurgical properties, such as abrasiveness. Special bench tests on rock drill cores are used in mapping the abrasiveness of rocks, with the Bond abrasion test being more commonly used in the mining industry, but it has a restrictive sampling protocol and mass requirement for geometallurgical studies. As a counterpoint, the test of the Laboratoire Central des Ponts et Chaussées/Central Laboratory of Bridges and Roads (LCPC) requires a smaller amount of fine material and a finer granulometric range. The study on the use of LCPC was implemented in 40 samples, using Bond Ai as a reference. The results showed a strong correlation between both methodologies (R^2 = 95%), validating the use of LCPC to quantify abrasiveness in the Sossego mine. It was also possible to classify the most abrasive lithologies.

Keywords: abrasiveness; geometallurgy; iron oxide-copper-gold ore; Bond abrasion test; LCPC

Citation: de Azevedo Barbosa, P.; Bergerman, M.G.; da Fonseca, E.; Kwitko-Ribeiro, R. Determination of Abrasiveness in Copper-Gold Sulfide Ores: A Contribution to the Geometallurgical Model of the Sossego Deposit. *Minerals* **2021**, *11*, 1427. https://doi.org/10.3390/min11121427

Academic Editors: Mehdi Parian, Pertti Lamberg and Marcos de Paiva Bueno

Received: 15 October 2021
Accepted: 3 December 2021
Published: 16 December 2021

1. Introduction

Abrasion is the most common wear mechanism in ore mining and mineral processing operations [1–8]. Albertin and Sinatora [2] pointed out the relationship between the abrasiveness of minerals and the wear of metal surfaces when their investigations showed that high-chromium white cast iron mill balls underwent faster wear when processing quartz instead of iron ore and phosphate rocks. Piazzetta et al. [9] and Moradizadeh et al. [10] also found that materials with high equivalent quartz content caused higher abrasion wear on metal surfaces. Proper quantification of the abrasiveness of different ores may be based on standardized tests. Such quantification in the mining industry is usually made through the Bond [1] test method, the preferred alternative among the various abrasion tests available [2,4–7,11]. The outcome of this test is the Bond abrasion index (Bond Ai), which finds widespread use among metallurgists and suppliers of consumables for crushers and mills as a parameter to estimate the expected wear of such consumables [4,6].

The Bond Ai test requires 1.6 kg of material with particle size ranging from 19.05 to 12.7 mm (3/4 to 1/2 in). In certain cases, such as studies in the early stages of a project or geometallurgical studies, where only drill core fragments or drilling chips are available, it may be difficult to get such an amount of material within the required size range.

Among the various ore abrasion measuring methods described by Peres [11] (p. 12), the LCPC test stands out for requiring finer material (between 6.3 and 4.0 mm) and just 0.5 kg of the sample [12,13].

Specific protocols and machinery are used for such tests, although they preserve the same rock-metal interaction mechanism. Notably, the LCPC test uses a small sample volume, fine-grained in a more restrictive range, which is subjected to high rotation on a relatively soft metal plate. In other words, it is a test formatted to measure any minimal contact caused by minerals and is, therefore, very sensitive. Bond Ai test subjects a sample about three times larger in particle size, with a coarser and wider grain size, and to a smoother rotational speed to wear a harder plate than used in the LCPC. Thus, Bond's Ai wear plate has little effect in the case of soft rocks compared to the LCPC.

Despite the strong correlation between the abrasiveness results by Bond Ai and by LCPC described in the literature, its equation needs to be confirmed for different ores/mines, since the particularities of rock and mineral typologies, and even the difference between the steel plates used in different laboratories, can affect the correlation [11,14,15].

Geometallurgical studies are widely used to help operations improve their profits [16–19]. For the Sossego mine, which includes the open pits—Sossego, Sequeirinho, and Pista—and an ore processing plant, geometallurgical studies [20–23] were carried out, mainly during the pre-feasibility and feasibility stages, extending over the first years of production (2004), until 2017. This historical geometallurgical database, totaling 135 samples, was obtained from exploratory drilling holes and submitted to bench tests for technological characterization of typical ores to support the definition of the appropriate process route, as well as the dimensioning of mine equipment for operational studies. Figure 1a illustrates the location of the total samples by lithology and by mining plan year for these geometallurgical historical data. The gray object in image "b" is the reference topography of December 2017.

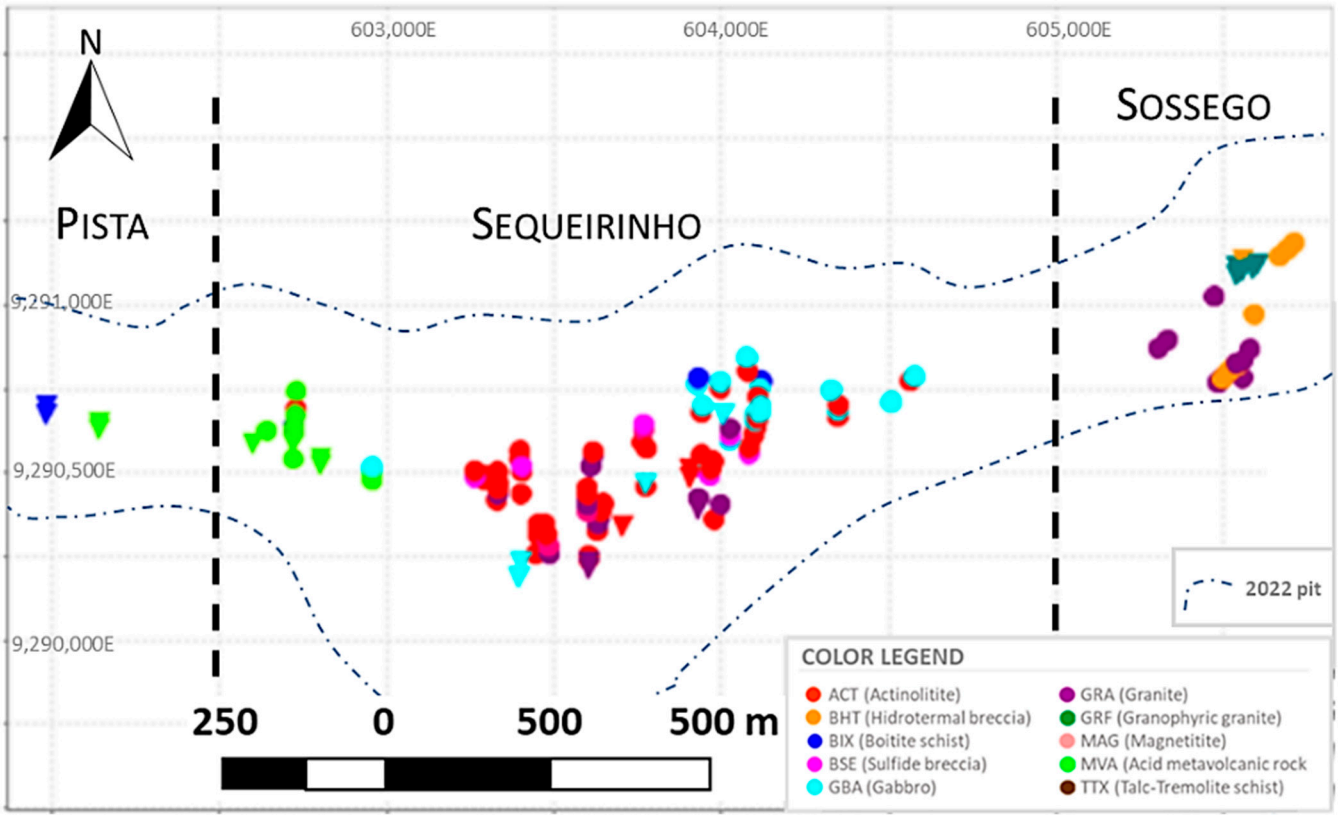

(**a**)

Figure 1. *Cont.*

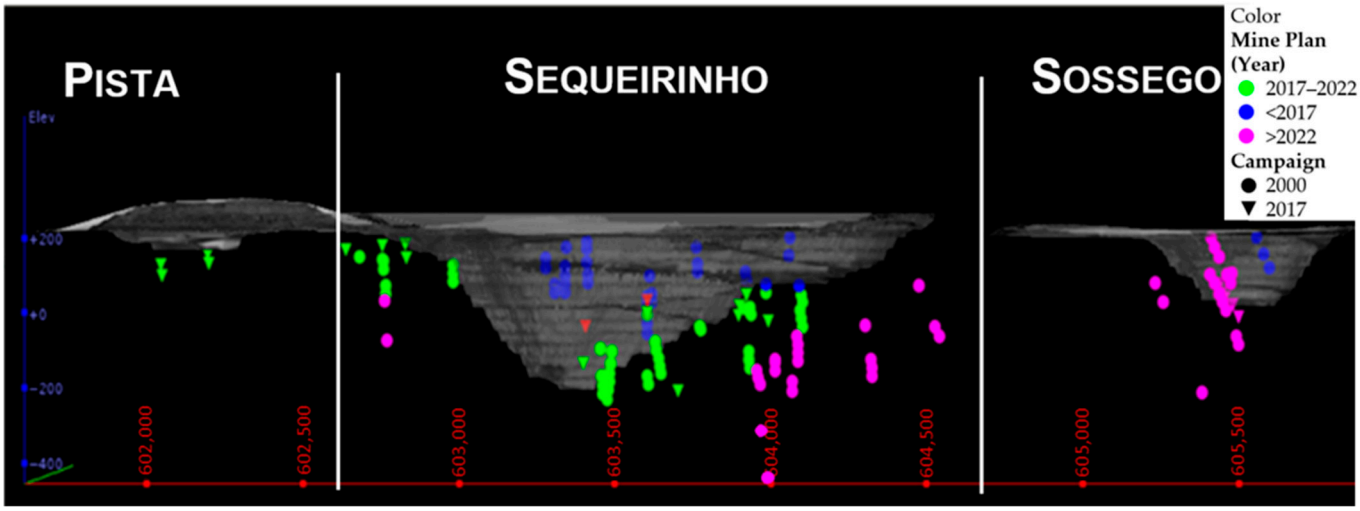

(**b**)

Figure 1. (**a**) 2D location map for Sossego's historical data with 135 samples at the Pista, Sequeirinho, and Sossego pits by lithology; (**b**) 3D view E–W to North direction of samples location by year of mining plan. The gray topography represents the pit as in 2017. The circle and triangle symbols on sample positions represent the two old campaigns carried out in 2000 and 2017, respectively.

These past studies at Sossego Mine [22] include a qualitative and quantitative mineralogy description, drop weight test (DWT), point load test (PLT), tumbler index (ta), SATMAGAN® (magnetic susceptibility), Bond work index (Wi), and the Bond abrasiveness index (Ai). The following lithology codes were used based on Vale procedures: ACT (actinolitite), BHT (hydrothermal breccia), BIX (biotite schist), BSE (Sequeirinho breccia), BSO (Sossego breccia), GBA (gabbro), GRA (granite), GRF (granophyric granite), MAG (magnetitite), MVA (metavolcanic acid), and TTX (talc-tremolite schist).

Only 60 samples were tested for Bond Ai, and a large range of abrasiveness values were found (Figure 2). A low representativity across the pits was considered due to not having samples on the Pista area between 2022–2024 (final pit) and having only a few samples at the bottom of Sequeirinho, until its lifetime in 2026. The low number of samples and the large range in values provides an opportunity to investigate this property again with new samples and methods to formulate new understandings. For the historical data [22], the MAG and TTX lithology groups were not tested by the Bond Ai and the breccia samples were distinguished by copper-gold sulfide ore from Sossego body (BSO), Sequeirinho body (BSE), and without ore (BHT).

In general, the graph in Figure 2 represents what is expected of the abrasive behavior of the rocks of the Sossego deposit, with a high variation of this property among the studied rocks. Although the MVA lithology had the highest abrasiveness average, some other lithologies had no expected high values, such as granitic types (GRA and GRF). The high silica [22–24] content is an answer for the MVA group, and almost all its occurrences are localized in a portion of Pista pit, at the west trend of the Sequeirinho body. Similar to the high values, the large ranges observed at almost all lithological groups were unsatisfactory for the establishment of future effective use. It caused a strong negative impact between January 2017 to the end of 2019, specifically for MVA processing. These feed changes resulted in a high cost in wear material consumption, increasing by 7% over the wear of SAG and ball mills screens and crusher liners. All these aspects made it necessary to carry out a new abrasiveness study for the Sossego deposit.

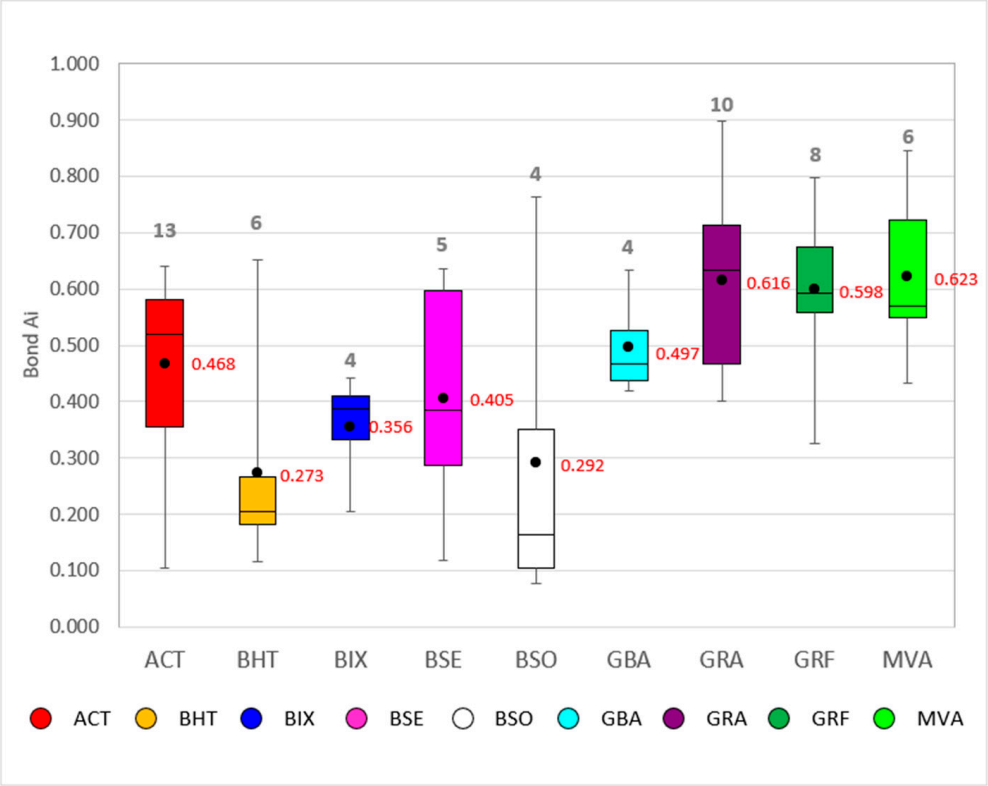

Figure 2. Statistic box plot graph of Bond Ai values with the sample quantity (except for MAG and TTX groups). The colors are standardized by lithology. The values above each bar are the number of samples and in the right position are the average.

In this study, 40 new samples from different areas of the Sossego, Sequeirinho, and Pista pits were characterized using the Bond and LCPC methodologies. The main objective was to validate the correlation between them so that the simplified LCPC test could be used for future geometallurgical studies and to identify the lithologies and mine domains with higher abrasion values.

No comparative study, including the historical data, could be carried out regardless of the authors' choice, given the differences in the type of samples used and uncertainties about the lithological classification protocols and the sample handling preparation applied for the Bond Ai of historical geometallurgical campaigns.

2. Materials and Methods

According to the planning of this sampling campaign, 40 new samples were randomly collected, representing the lithological diversity of the mineral deposit and the study's objectives. These samples were identified with the initials AMPT, followed by a sequential number. Thus, the eight main lithologies distributed in three pits were considered, as seen in the map in Figure 3. Some of these samples were collected from blasted outcrops inside the pits, represented on the map by yellow points, and another group of samples was collected from temporary ore stockpiles at red points.

The lithologies were coded, following the same procedures described in Section 1: ACT, BIX, BSE, GRA, GRF, MAG, MVA, and TTX. The MVA was preferentially sampled based on the preliminary information from the processing plant about its high abrasiveness. However, the campaign comprised only two samples for ACT because its occurrence was limited. The BHT of historical data was the same texture and mineral assemblage as BSE in this study.

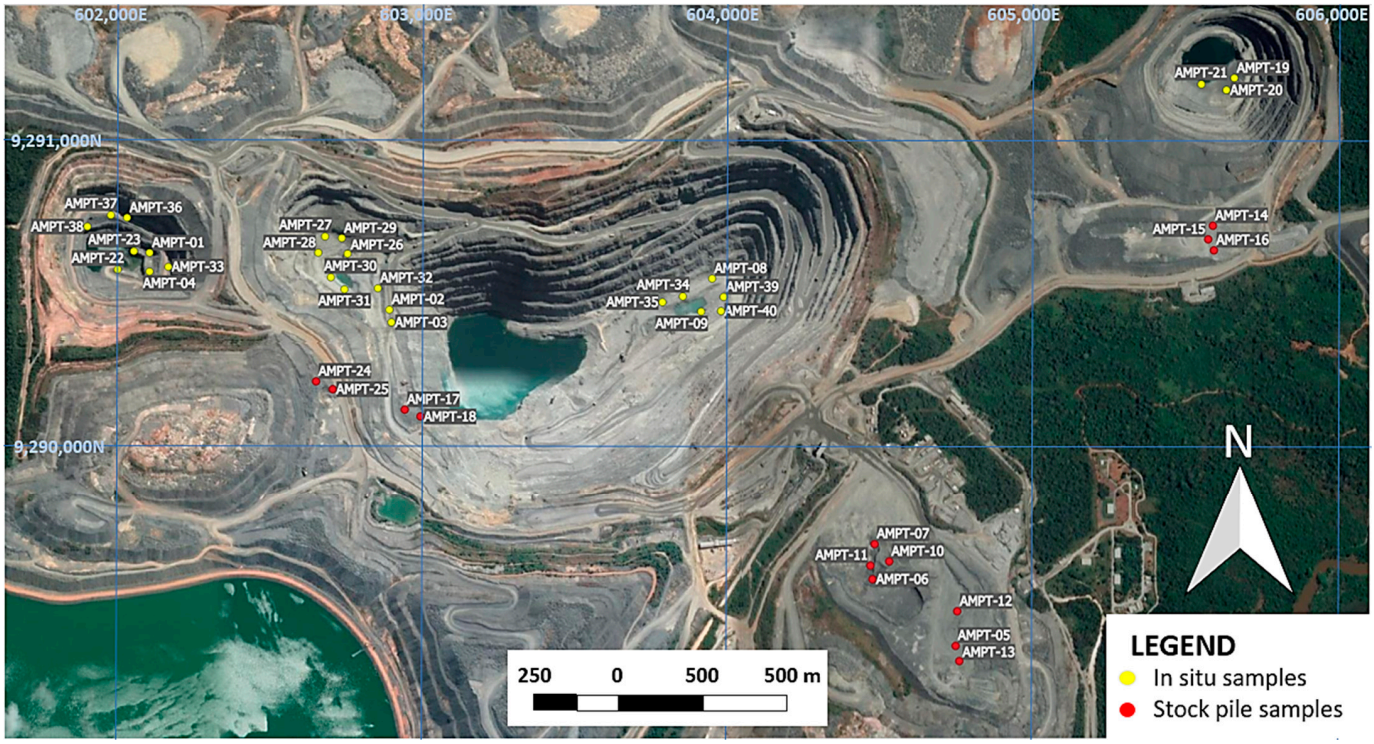

Figure 3. Location map of 40 new samples. Yellow targets for in situ samples and the red targets for samples transported from their origin [25]. Reference image from 07 August 2021.

The samples, weighing around 5–7 kg and between 75 and 10 mm in size, were stage crushed in a jaw crusher until 100% below 19.05 mm and classified between 19.05 and 12.7 mm. Four 400 g aliquots were prepared from each sample for the Bond test and one 1 kg aliquot was taken for the LCPC test, ensuring that both tests would be conducted on mineralogically similar materials. The LCPC aliquots were subsequently stage crushed in a jaw crusher until 100% below 6.3 mm and above 4.0 mm.

The LCPC test was carried out according to the French Standard P18–579 [13]. The test measures the mass loss of a metal plate with 50 mm × 25 mm × 5 mm in size that rotates for 5 min at 4500 rpm in contact with 500 g of material at the specified size range between 6.3 and 4.0 mm. The plate is made from low carbon steel (C1015), with Rockwell hardness from 60 HRB to 75 HRB. The LCPC abrasiveness index is determined according to Equation (1):

$$\text{LCPC (g/t)} = 1000 \times 1000\ (\text{Mip} - \text{Mfp})/\text{M}, \quad (1)$$

where:

Mip—plate mass before to the LCPC test;
Mfp—plate mass after the LCPC test;
M—sample mass (500 ± 0.2 g)

The Bond test follows the protocol proposed by Bond [1], according to which four 400 g samples are processed for 15 min in a Bond's abrasion tester. The material abrasiveness is calculated from the wear of a 500-Brinel hardened SAE 4325 steel plate/implement fitted inside the equipment according to Equation (2).

$$\text{Ai (g)} = \text{Mi} - \text{Mf}, \quad (2)$$

where:

Ai—Bond abrasion index;
Mi—initial steel plate mass;
Mf—final steel plate mass.

The hardness of all metal plates was measured using a Rockwell Hardness Tester (manufactured by Wilson, New York, NY, USA) to ensure their hardness met the applicable requirements [1,13]. Such measurement indicated that the LCPC test plates had a 65 HRB average hardness, falling within the range as defined by the French standard [13]. The hardness test result for the plates used in the Bond test was 525 HB, close to the 500 HB hardness specified by Bond [1]. The plates were from the same lot and manufacturer in all tests, aimed at preventing possible manufacturing variations from affecting the test results. The mineralogy of the final product ground was measured to confirm the similarity between the samples used in LCPC and Bond Ai and used to classify lithologies, sample by sample.

For the mineralogical characterization, polished sections were produced, following a proprietary method of cold epoxy embedding under centrifugation [26]. The preparation with sample to epoxy ratio of 1:2 (vol.) was centrifuged, demolded, cut along the vertical axis, and potted again in a 30 mm round mold to ensure the representativeness of a single surface in terms of morphology, size, density, and particles' composition. The modal mineralogy was generated by the system QEMSCAN® (Quanta 650W, manufactured by FEI, Brisbane, Australia) of SEM-based automatized mineralogy, consisting of a FEI Quanta 650 SEM (manufactured by FEI, Brisbane, Australia) with two Bruker XFlash 6|30 EDS (manufactured by Bruker, Brisbane, Australia) detectors. All measurements were produced in the Field Image mode, under 25 kV of beam acceleration and 10 nA of sample current, using 15 µm × 15 µm of pixel spacing and 1500 X-ray counts per pixel. An average of 2 million pixels per sample were then generated, 30% of which were identified as mineral phases.

The chemistry of major elements was determined by infrared absorption, thermal conductivity with direct combustion (S), and inductively coupled plasma (ICP-OES, model, manufactured by Agilent, model5110, Victoria, Australia) with solubilization in aqua regia (Cu), solubilization in HNO_3 + HF (K and Na), and calcination at 600 °C with fusion in $Na_2CO_3/Na_2B_4O_7$ (Ca, Fe, and Si).

3. Results

The results comprise an initial and determinant validation that aims to guarantee the tests reproducibility and the similarity between the pairs of the 40 new tested samples. The statistical study defined the lithological composition of the samples and mathematically represented the abrasiveness property.

3.1. Validations

A quality control campaign was implemented using five duplicate samples to evaluate the reproductivity of the Bond Ai and LCPC tests. Only the sample AMPT-30 showed a deviation greater than 15%; however, this was not significant due to their low values at around zero. All the samples were within the expected range, below 10% and, therefore, acceptable (Table 1).

The preliminary visual lithological classification was confirmed through mineralogical evaluation. Assay reconciliation (Figure 4) allows to compare QEMSCAN® calculated chemical data obtained from mineral chemistry with externally measured chemical data and is used for validation of mineralogical data. The data are plotted against one another on the chart for visual comparison and identification of potentially anomalous measurements. A slight dispersion from 1:1 regression, as observed in the graph, is expected and is due to fluctuations in mineral chemistry from an average stoichiometry.

The small cloud dispersion and the trendline inclination (Figure 5), using the LCPC and Bond Ai values, could reinforce the effectiveness of the sample preparation methodology using just the six major mineral types. These analyses satisfied the primary requirement of similarity between the tested pairs and confirmed the lithological classifications.

Table 1. Results of duplicate samples.

Sample	Test Type	Samples No.	Average	Relative Error
AMPT-11	Bond Ai	3	0.490	8.16%
	LCPC	3	1192	2.35%
AMPT-18	Bond Ai	2	0.245	6.12%
	LCPC	2	830	1.75%
AMPT-21	Bond Ai	2	0.225	2.22%
	LCPC	2	863	5.91%
AMPT-23	Bond Ai	2	0.700	0.00%
	LCPC	2	1441	0.94%
AMPT-30	Bond Ai	2	0.015	33.33%
	LCPC	2	111	10.41%

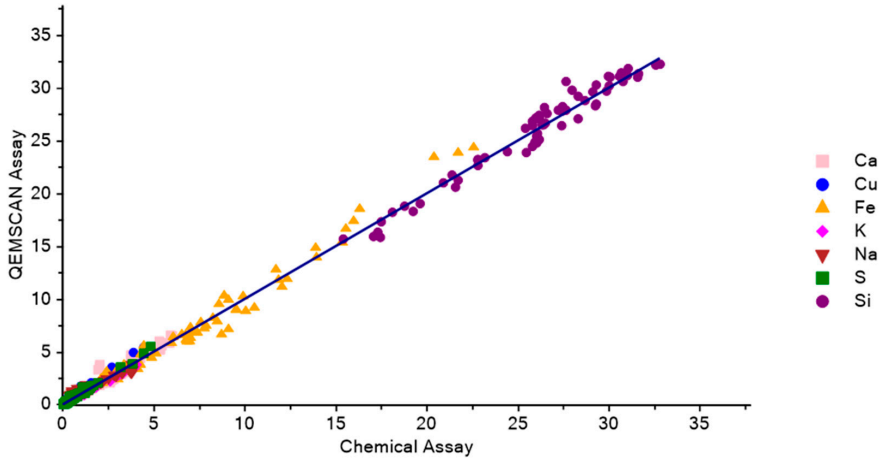

Figure 4. QEMSCAN® assay reconciliation of the 72 measured samples. The 1:1 trendline is in blue.

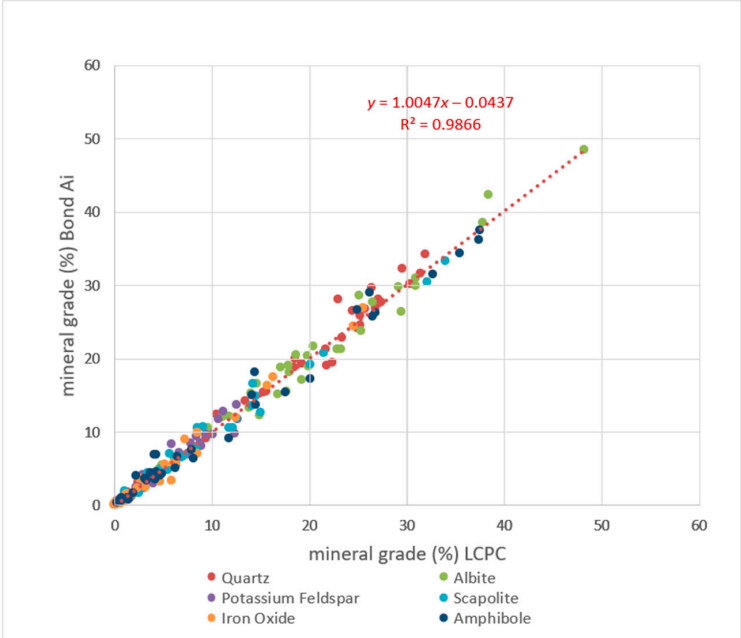

Figure 5. Mineralogy results for the six major mineral groups sampled for LCPC and Bond Ai.

Charts for each pair of samples in Supplementary Materials (Figures S1–S36) summarize graphs of mineralogical analysis from QEMSCAN® data used for lithological classification, such as horizontal bars and scatterplot of the mineral percent, in addition to microscopic images with the mineralogical assemblage. The first four samples were not part of the analysis, maintaining the mineralogical field classification.

3.2. Lithological Study

The database in Table 2 includes the 40 new samples, each one with its coded lithology, distinguished by two sets of raw values of abrasiveness (non-normalized measured values) acquired in these tests. The results show a wide variation of abrasiveness, compatible with the expected hardness for the analyzed lithologies, whereas the value ranges are from 0.006 to 0.770 for Bond Ai and from almost 0 to 1490 for LCPC, suggesting high abrasiveness.

Table 2. List of sample results and lithological classification.

Sample	Lithology	Bond Ai	LCPC	Sample	Lithology	Bond Ai	LCPC
AMPT-01	MVA	0.674	1394	AMPT-21	GRF	0.220	914
AMPT-02	MVA	0.532	1278	AMPT-22	MVA	0.770	1490
AMPT-03	MVA	0.545	1269	AMPT-23	MVA	0.700	1427
AMPT-04	MVA	0.520	1304	AMPT-24	BIX	0.260	768
AMPT-05	MVA	0.260	939	AMPT-25	MVA	0.510	1203
AMPT-06	MVA	0.510	1143	AMPT-26	MVA	0.570	1287
AMPT-07	ACT	0.390	956	AMPT-27	BIX	0.280	849
AMPT-08	ACT	0.330	817	AMPT-28	MVA	0.580	1289
AMPT-09	BSE	0.340	941	AMPT-29	MAG	0.370	850
AMPT-10	MVA	0.420	1035	AMPT-30	TTX	0.020	99
AMPT-11	MVA	0.490	1222	AMPT-31	TTX	0.006	31
AMPT-12	BIX	0.210	731	AMPT-32	MVA	0.720	1379
AMPT-13	BSE	0.370	1089	AMPT-33	MVA	0.620	1395
AMPT-14	GRA	0.310	981	AMPT-34	BIX	0.280	808
AMPT-15	GRA	0.330	966	AMPT-35	BIX	0.160	656
AMPT-16	GRA	0.380	970	AMPT-36	BIX	0.100	405
AMPT-17	MVA	0.600	1303	AMPT-37	BIX	0.140	685
AMPT-18	BSE	0.230	844	AMPT-38	MAG	0.360	874
AMPT-19	GRF	0.250	813	AMPT-39	MAG	0.430	1037
AMPT-20	GRF	0.270	884	AMPT-40	BIX	0.240	914

A visualization of all datasets is presented in the box plot of Figure 6 below based on the lithology variable. Most of the lithologies do not have extensive tails, and the most discrepant outliers are in the MVA lithology, which is explained by its heterogeneity and mineral assemblage. The layers formed on the MVA, with felsic bands of dominant quartz and feldspar at odds with mafic bands composed mainly of amphibole/actinolite, biotite, and scapolite, could represent this variability.

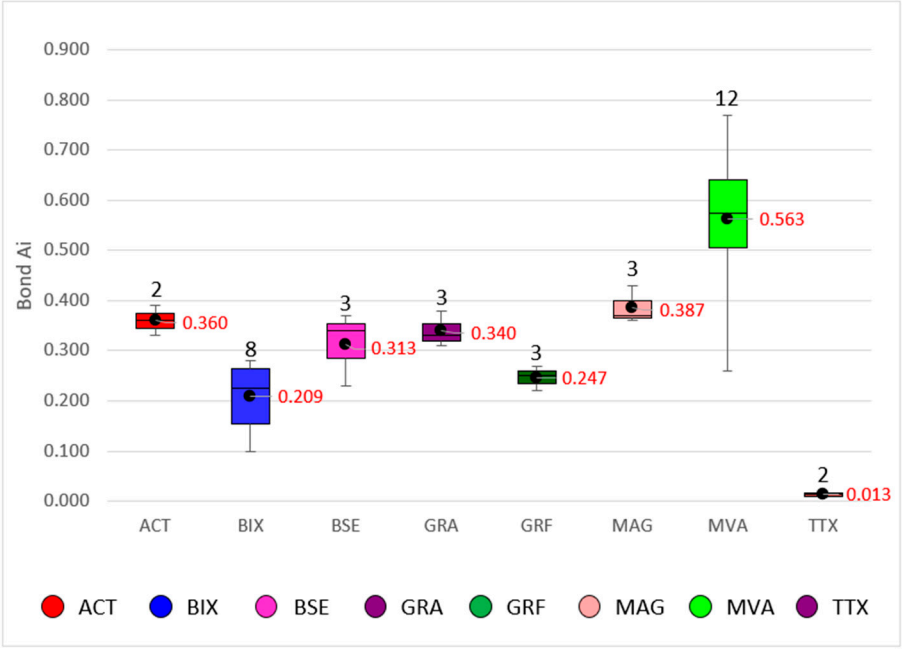

(**a**)

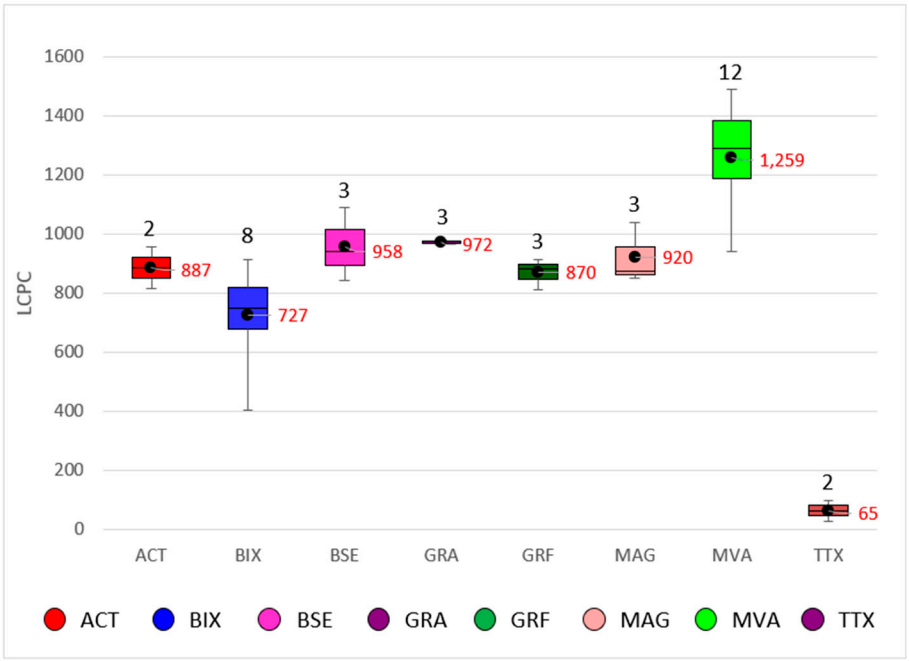

(**b**)

Figure 6. Results from new abrasiveness datasets with box plot by lithology for (**a**) Bond Ai; (**b**) LCPC. The colors are standardized by lithology. The values above each bar are the number of samples and in the right position are the average.

3.3. Statistical Analysis

The statistical summary by lithology is shown in Table 3. The TTX (high talc) lithology had the lowest values for Bond Ai (mean and median of 0.013) and LCPC (mean and median of 65), with the highest values seen in the MVA lithology (mean and median of Bond Ai around 0.570 and LCPC around 1288).

Table 3. Statistical summary of test results for the entire sample population and by lithology.

Stats		Bond Ai	LCPC	Stats		Bond Ai	LCPC	Stats		Bond Ai	LCPC
Global		40	40	BSE	Count Num	3	2	MAG	Count Num	3	2
Minimum		0.006	31	BSE	Minimum	0.230	844	MAG	Minimum	0.360	850
Maximum		0.770	1490	BSE	Maximum	0.370	1089	MAG	Maximum	0.430	1037
Mean		0.382	981	BSE	Mean	0.313	958	MAG	Mean	0.387	920
Median		0.365	961	BSE	Median	0.340	941	MAG	Median	0.370	874
Stand Dev		0.189	327	BSE	Stand Dev	0.074	123	MAG	Stand Dev	0.038	102
Coeff var		49.52	33.30	BSE	Coeff var	23.52	12.88	MAG	Coeff var	9.79	11
ACT	Count Num	2	2	GRA	Count Num	4	2	MVA	Count Num	15	2
ACT	Minimum	0.330	817	GRA	Minimum	0.310	966	MVA	Minimum	0.260	939
ACT	Maximum	0.390	956	GRA	Maximum	0.420	1035	MVA	Maximum	0.770	1490
ACT	Mean	0.360	887	GRA	Mean	0.360	988	MVA	Mean	0.573	1288
ACT	Median	0.360	887	GRA	Median	0.355	976	MVA	Median	0.570	1289
ACT	Stand Dev	0.042	98	GRA	Stand Dev	0.050	32	MVA	Stand Dev	0.122	133
ACT	Coeff var	11.78	11.09	GRA	Coeff var	13.80	3.245	MVA	Coeff var	21.25	10.30
BIX	Count Num	8	8	GRF	Count Num	3	3	TTX	Count Num	2	2
BIX	Minimum	0.100	405	GRF	Minimum	0.220	813	TTX	Minimum	0.006	31
BIX	Maximum	0.280	914	GRF	Maximum	0.270	914	TTX	Maximum	0.020	99
BIX	Mean	0.208	727	GRF	Mean	0.247	870	TTX	Mean	0.013	65
BIX	Median	0.225	750	GRF	Median	0.250	884	TTX	Median	0.013	65
BIX	Stand Dev	0.068	155	GRF	Stand Dev	0.025	52	TTX	Stand Dev	0.010	48
BIX	Coeff var	32.73	21.35	GRF	Coeff var	10.20	5.96	TTX	Coeff var	76.15	73.97

A principal component analysis was on Figure 7 and performed to evaluate the mineralogical assemblage and abrasiveness behavior (LCPC), where it can be seen that, in addition to quartz, other minerals showed a strong correlation with abrasiveness, such as albite, biotite, talc, and scapolite.

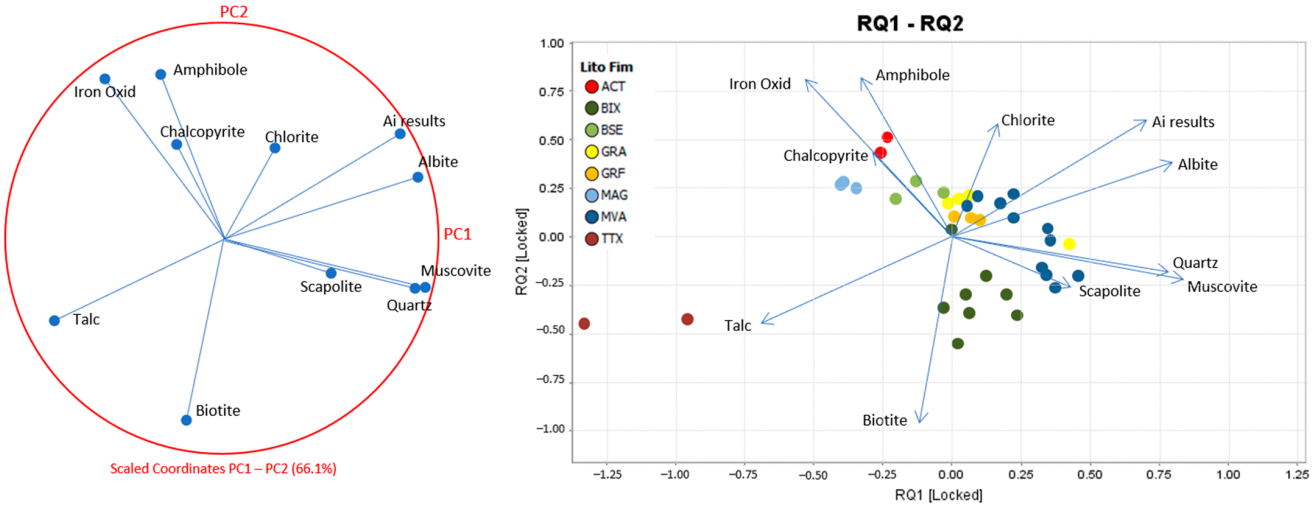

Figure 7. Principal component analysis of minerals categorized by lithology from ioGAS™ software.

Table 4 shows a correlation matrix between the 12 minerals and the LCPC values, in which the highest correlation could be seen at a value of 0.73 for albite, followed by scapolite, muscovite and quartz. It still confirms the low correlation with the talc mineral.

Table 4. Correlation matrix from ioGAS™ software [27] showing the correlation between the minerals and LCPC.

Correlation	LCPC	Quartz	Albite	K-feldspar	Muscovite	Scapolite	Biotite	Chlorite	Talc	Amphibole	Fe-Oxides	Apatite	Carbonate
LCPC	1	0.37	0.73	0.29	0.38	0.52	−0.64	0.033	−0.68	0.033	−0.087	−0.071	0.074
Quartz	0.37	1	0.35	0.58	0.6	0.12	0.08	0.39	−0.42	−0.75	−0.61	−0.55	0.43
Albite	0.73	0.35	1	0.33	0.43	0.1	−0.45	0.1	−0.42	−0.22	−0.38	−0.24	0.037
K-feldspar	0.29	0.58	0.33	1	0.42	−0.2	−0.3	0.58	−0.37	−0.35	−0.33	−0.062	0.53
Muscovite	0.38	0.6	0.43	0.42	1	0.44	0.17	−0.16	−0.36	−0.54	−0.62	−0.45	−0.14
Scapolite	0.52	0.12	0.1	−0.2	0.44	1	−0.12	−0.57	−0.21	−0.064	−0.049	−0.19	−0.37
Biotite	−0.64	0.08	−0.45	−0.3	0.17	−0.12	1	−0.29	0.24	−0.35	−0.35	−0.31	−0.24
Chlorite	0.033	0.39	0.1	0.58	−0.16	−0.57	−0.29	1	−0.24	−0.14	−0.14	0.13	0.7
Talc	−0.68	−0.42	−0.42	−0.37	−0.36	−0.21	0.24	−0.24	1	−0.17	0.046	−0.16	−0.14
Amphibole	0.033	−0.75	−0.22	−0.35	−0.54	−0.064	−0.35	−0.14	−0.17	1	0.73	0.68	−0.21
Fe-Oxides	−0.087	−0.61	−0.38	−0.33	−0.62	−0.049	−0.35	−0.14	0.046	0.73	1	0.48	−0.12
Apatite	−0.071	−0.55	−0.24	−0.062	−0.45	−0.19	−0.31	0.13	−0.16	0.68	0.48	1	−0.083
Carbonate	0.074	0.43	0.037	0.53	−0.14	−0.37	−0.24	0.7	−0.14	−0.21	−0.12	−0.083	1

3.4. Mathematical Correlation

The relationship between Bond Ai and LCPC can be studied through dispersion diagrams, which are used to demonstrate this correlation. Two trendlines in Figure 8 represent different correlations. The data lie closer to a quadratic polynomial equation (blue) than a linear trend (red), increasing the determination coefficient (R^2) from 87.70% to 94.57%.

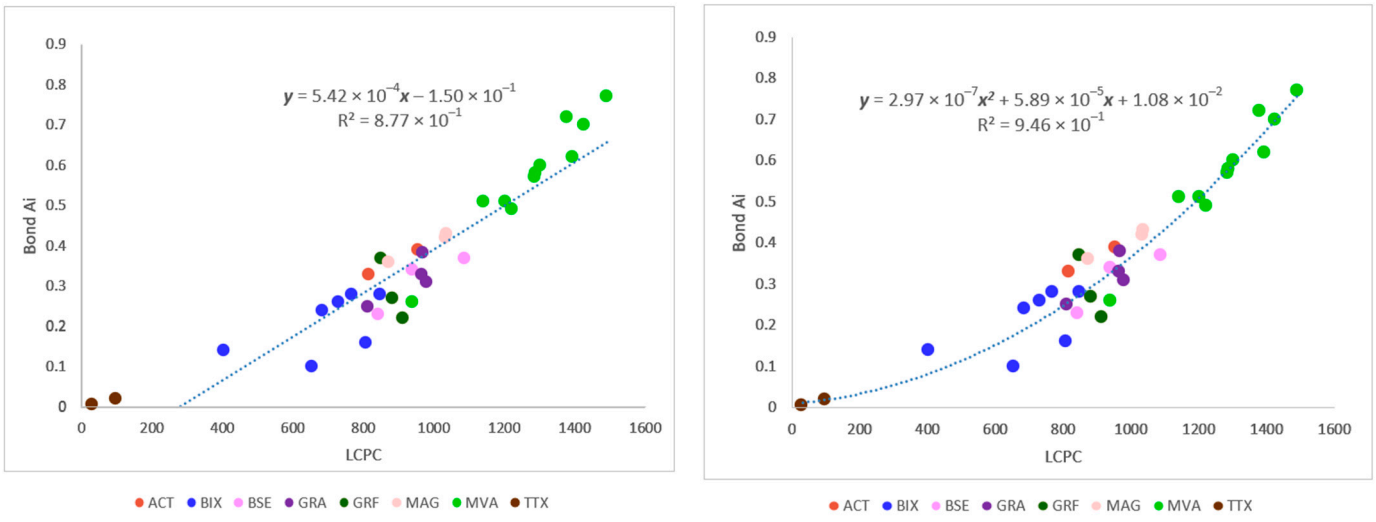

(**a**) (**b**)

Figure 8. Correlation graphs LCPC versus Bond Ai for the total set of samples from the Sossego deposit. The dots are colored according to their lithologies and expose different correlations: (**a**) linear and (**b**) quadratic.

Table 5 for a summary of statistical results including analysis of variance to the regression and to the predictive model for Bond Ai based on LCPC values shows a constant variance for residues, and the zero *p*-value, validating the equation.

Table 5. Statistic output table with summary of equation results and the residue analysis for the predictive model for Bond Ai based on LCPC values from Minitab® software [28].

Model Summary			Analysis of Variance						Analysis of Variance				
S	**R-sq**	**R-sq(ad)**	**Source**	**DF**	**SS**	**MS**	***f*-Value**	***p*-Value**	**Source**	**DF**	**SS**	***f*-Value**	***p*-Value**
0.0449929	94.57%	94.24%	Regression	4	1.16399	0.581995	287.50	0.000	Linear	1	1.07937	242.36	0.000
–	–	–	Error	33	0.06680	0.002024	–	–	Quadratic	1	0.08462	41.80	0.000
–	–	–	Total	35	1.23080	–	–	–	–	–	–	–	–

A residue analysis was performed to prove the quadratic correlation, observing a normal distribution and a symmetric histogram (Figure 9).

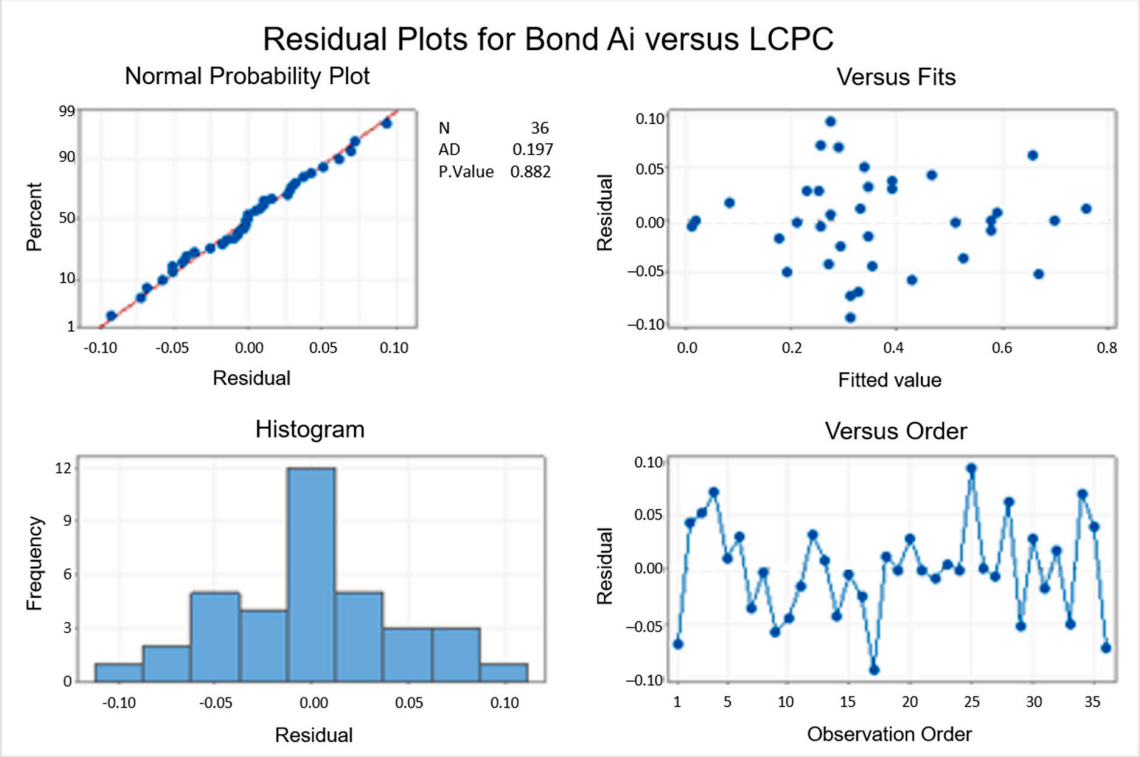

Figure 9. Residue graphs from Bond Ai versus LCPC at normal fitted and a symmetric histogram from Minitab® software [28].

According to the validations for this database, both tests (Bond Ai and LCPC) represent the same phenomenon of abrasion wear with a high (above 94.57%) correlation index.

Therefore, the Bond Ai forecast for a given value of LCPC for the copper-gold of the Sossego deposit can be described by the following Equation (3):

$$Y = 2.97 \times 10^{-7}x^2 + 5.89 \times 10^{-5}x + 1.08 \times 10^{-2}, R^2 = 0.95, \quad (3)$$

where:

Y—Bond Ai value;
x—LCPC value;

An additional regression analysis was done to predict the LCPC value from the mineral content, establishing their direct correlation. A multiple regression Equation (4) was obtained to estimate consideration of the most significant minerals, such as quartz, biotite, albite, and chlorite. They were transformed into logarithms, as shown below (Table 6).

$$\text{LCPC} = 980 - 446 \log.\text{biotite} + 286 \log.\text{albite} - 427 \log.\text{chlorite} + 333 \log.\text{quartz}, \quad (4)$$

where:

biotite—biotite mineral grade;
albite—albite mineral grade;
chlorite—chlorite mineral grade;
quartz—quartz mineral grade.

Table 6. Multiple regression to predict the LCPC values based on mineralogy.

Coefficients						Model Summary				Analysis of Variance					
Team	**Coef**	**SE Coef**	***t*-Value**	***p*-Value**	**VIF**	**S**	**R-sq**	**R-sq(ad)**	**R-sq(pred)**	**Source**	**DF**	**Adj SS**	**Adj MS**	***f*-Value**	***p*-Value**
Constant	980	124	7.91	0.000	–	113.511	89.11%	87.71%	85.48%	Regression	4	3,269,216	817,304	63.43	0.000
log biotite	−446.1	643	−6.94	0.000	2.25	–	–	–	–	log biotite	1	620,292	620,292	48.14	0.000
log albite	286	107	2.67	0.012	4.55	–	–	–	–	log albite	1	92,080	92,080	7.15	0.012
log chlorite	−426.7	76.7	−5.56	0.000	1.29	–	–	–	–	log chlorite	1	398,893	398,893	30.96	0.000
log quartz	332.6	84.8	3.92	0.000	4.19	–	–	–	–	log quartz	1	198,048	198,048	15.37	0.000
–	–	–	–	–	–	–	–	–	–	Error	31	399,428	12,885	–	–
–	–	–	–	–	–	–	–	–	–	Total	35	3,668,643	–	–	–

The adjusted determination coefficient was 87.71%, and the residue analysis revealed a normal distribution, symmetric histogram, with a very low *p*-value and constant variance for the residues (Figure 10), validating Equation (4).

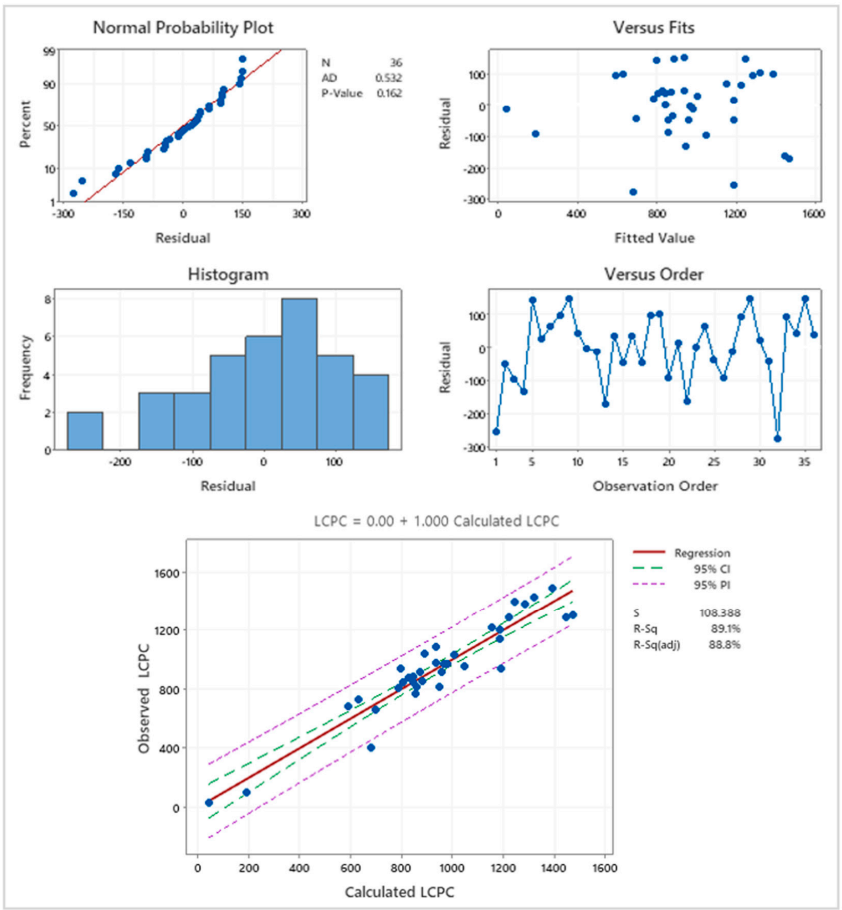

Figure 10. Statistical regression from Minitab® [28] to residue analysis on the left top, the correlation between observed versus calculated values of LCPC on the right top and fitted line plot from LCPC data on the bottom.

4. Conclusions

The results of the abrasiveness index for the Sossego mine show that abrasiveness varies significantly depending on the lithology, with the MVA being the highest. This information will allow the operation and process team at the Sossego plant to take preventive measures to minimize the impact of processing this highly abrasive material. The validation of the methodology confirmed the similarity of the samples used in the Bond Ai and LCPC tests. The validation also showed that both tests have a low deviation, less than 10%, and the LCPC has an even smaller deviation than Bond's Ai. Finally, this study demonstrated the correlation between Bond Ai and LCPC for the Sossego deposit, thus validating its use for abrasive geometallurgical studies. Such correlation can be validated for other deposits, thus allowing generalized use for geometallurgical studies.

Throughout the work, the observations regarding the variations between the tests pointed to the non-linearity for such aspects: distinct sample support between the tests (mass and grain size interval), different test protocols (rotation speed and residence time), different mechanism of the particle's trajectory inside the respective bowl, and difference in hardness between the standard metal plates of the two tests.

Such results validate the use of the LCPC for geometallurgical studies of the Sossego mine and represent an opportunity for further research, as well as applications aimed at improving the understanding of the LCPC test and its correlation with Bond's Ai for different ores, despite the industry availability of other tests aimed at measuring abrasiveness in rocks.

Supplementary Materials: The following are available online at https://www.mdpi.com/article/10.3390/min11121427/s1, Figures S1–S36 include the detailed results of the mineralogical analysis of the samples used for Ai and LCPC tests, including the quantitative mineralogy, the QEMSCAN® images, and a correlation graph of the mineral grade results for each pair of samples.

Author Contributions: Conceptualization, P.d.A.B. and M.G.B.; methodology, P.d.A.B.; software, P.d.A.B. and R.K.-R.; validation, P.d.A.B., M.G.B. and E.d.F.; formal analysis, P.d.A.B.; investigation, P.d.A.B.; resources, P.d.A.B. and M.G.B.; data curation, P.d.A.B.; writing—original draft preparation, P.d.A.B., M.G.B., E.d.F. and R.K.-R.; writing—review and editing, P.d.A.B.; visualization, P.d.A.B., M.G.B., E.d.F. and R.K.-R.; supervision, M.G.B.; project administration, P.d.A.B. and M.G.B.; funding acquisition, M.G.B. All authors have read and agreed to the published version of the manuscript.

Funding: The abrasiveness tests were carried out through a partnership between VALE-ITV/USP within the Min-AO2 project, Systemic Management of Mine Planning, and Operation at the Mine of the Future, using equipment and labor from the Treatment Laboratory LTM-Poli/USP ore and at Vale's physicochemical laboratories, supported under the Universal CNPQ Project No. 449932/2014-1 and research grant CT2016—308767/2016-0.

Data Availability Statement: The geological data and the samples collected, the basis that supported the results, come from the Vale SA Company. Their availability was previously authorized upon consent from the company and through a partnership to finance of the aforementioned project; therefore, the results are not included in its corporate statements in the public domain.

Acknowledgments: The authors would like to thank the University of Sao Paulo's Mineral Engineering Post-Graduate Program supported by Maurício Bergerman and the Vale geologist/geometallurgical team, represented by Elisabeth da Fonseca and Rogério Kwitko, for supporting this research project.

Conflicts of Interest: The authors declare no conflict of interest.

Nomenclature

IOCG	Iron Oxide Copper and Gold
LCPC	Laboratoire Central des Ponts et Chaussées
DWT	Drop weight test
PLT	Point load test
ta	Tumbler index
SATMAGAN®	Magnetic susceptibility

Wi	Bond work index
Ai	Bond abrasiveness index
ACT	Actinolitite
BHT	Hydrothermal breccia
BIX	Biotite schist
BSE	Sequeirinho breccia
BSO	Sossego breccia
GBA	Gabbro
GRA	Granite
GRF	Granophyric granite
MAG	Magnetitite
MVA	Metavolcanic acid
TTX	Talc-tremolite schist
AMPT	Sample identification
HRB	Rockwell Hardness B
HB	Brinell Hardness
QEMSCAN®	Qualitative evaluation of minerals by scanning electron microscopy
SEM	Scanning electron microscopy
EDS	Energy-dispersive spectrometry
ICP-OES	Inductively coupled plasma—optical emission spectrometry
PC	Principal component
S	Standard deviation of the distance between data and fitted values
R sq	Coefficient of determination
R sq(ad)	Adjusted coefficient of determination
R sq(pred)	Predicted coefficient of determination
DF	Total degrees of freedom
SS	Sum of squares
MS	Mean squares
f-Value	Statistic test used to determine whether the term is associated with the response
p-Value	Probability that measures the evidence against the null hypothesis
t-Value	Ratio between the coefficient and its standard error
SE Coef	Standard error of the coefficient
VIF	Variance inflation factor
Adj SS	Adjusted sum of squares
Adj MS	Adjusted mean squares

References

1. Bond, F.C. Metal wear in crushing and grinding. In Proceedings of the LIV Annual Meeting of The American Institute of Chemical Engineering, Houston, TX, USA, 3 December 1963; p. 90.
2. Albertin, E.; Sinatora, A. Effect of carbide fraction and matrix microstructure on the wear of cast iron balls tested in a laboratory ball mill. *Wear* **2001**, *250*, 492–501. [CrossRef]
3. Rendón, J.; Olsson, M. Abrasive wear resistance of some commercial abrasion resistant steels evaluated by laboratory test methods. *Wear* **2009**, *267*, 2055–2061. [CrossRef]
4. Giblett, A.; Siedel, J. Measuring, predicting and managing grinding media wear. Paper No. 34. In *Conference on International Autogenous Grinding, Semi-Autogenous Grinding Technology 2011*; Mining and Mineral Process Engineering, University of British Columbia: Vancouver, BC, USA, 2011.
5. Drucker, P. Validity of the LCPC abrasivity coefficient through the example of a recent Danube gravel. *Geomech. Tunn.* **2011**, *4*, 681–691. [CrossRef]
6. Massola, C.P.; Chaves, A.P.; Albertin, E. A discussion on the measurement of griding media wear. *J. Mater. Res. Technol.* **2016**, *5*, 282–288. [CrossRef]
7. Morrell, S. Testing and calculations for comminution machines. In *SME—Mineral Processing and Extractive Metallurgy Handbook*; Society for Mining, Metallurgy and Exploration Press: Englewood, CO, USA, 2019.
8. Svanberg, A.; Larsson, S.; Mäki, R.; Jonsén, P. Minerals full–scale simulation and validation of wear for a mining rope shovel bucket. *Minerals* **2021**, *11*, 623. [CrossRef]
9. Piazzetta, G.R.; Lagoeiro, L.E.; Figueira, I.F.R.; Rabelo, M.A.G.; Pintaude, G. Identification of abrasion regimes based on mechanisms of wear on the steel stylus used in the Cerchar abrasiveness test. *Wear* **2018**, *410*, 181–189. [CrossRef]
10. Moradizadeh, M.; Cheshomi, A.; Ghafoori, M.; Tarighazali, S. Correlation of equivalent quartz content, slake durability index and Is50 with Cerchar abrasiveness index of different types of rock. *Int. J. Rock Mech. Min. Sci.* **2016**, *86*, 1591–1596. [CrossRef]

11. Peres, L.M. Avaliação da Abrasividade de Minérios a Partir do Ensaio LCPC Como Alternativa ao Método de Bond. Bachelor's Thesis, Universidade de Paulo, São Paulo, Brazil, 2017.
12. Käsling, H.; Thuro, K. Rock mechanics in civil and environmental engineering: Determining rock abrasivity in the laboratory. In *Eurock 2010*; CRC Press: New York, NY, USA, 2010.
13. Norme FRANÇAISE P18–579. *Roches—Détérmination du Pouvoir Abrasive d'une Roche. Partie 1. Essai de Rayure Avec une Pointe*; AFNOR Association Française de Normalisation: Paris, France, 1990.
14. Metso. *Crushing and Screening Handbook*, 3rd ed.; Metso: Helsinki, Finland, 2008.
15. Freitas, L.S. Avaliação de Minérios Itabiritos Compactos e Semi–Compactos em um Circuito de Britagem da Samarco Mineração S/A. Master's Thesis, Universidade Federal de Minas Gerais, Belo Horizonte, Brazil, 2014.
16. Dominy, S.C.; O'connor, L.; Parbhakar–Fox, A.; Glass, H.J.; Purevgerel, S. Geometallurgy—A route to more resilient mine operations. *Minerals* **2018**, *8*, 560. [CrossRef]
17. Mwanga, A.; Rosenkranz, J.; Lamberg, P. Development and experimental validation of the Geometallurgical Comminution Test (GCT). *Miner. Eng.* **2017**, *108*, 109–114. [CrossRef]
18. Díaz, E.; Voisin, L.; Kracht, W.; Montenegro, V. Using advanced mineral characterization techniques to estimate grinding media consumption at laboratory scale. *Miner. Eng.* **2018**, *121*, 180–188. [CrossRef]
19. Bhuiyan, M.; Esmaieli, K.; Ordóñez-Calderón, J.C. Application of data analytics techniques to establish geometallurgical relationships to bond work index at the Paracutu Mine, Minas Gerais, Brazil. *Minerals* **2019**, *9*, 302. [CrossRef]
20. Bergerman, M.G.; Morais, J.; Castro, A.; Rosa, M.A.N.; Delboni Júnior, H. Variability studies for the Sossego 41 ktpd grinding circuit. In Proceedings of the XXIV International Mineral Processing Congress, Beijing, China, 24–28 September 2008; pp. 407–416.
21. Delboni, H.; Chieregati, A.; Bergerman, M. Development and validation of ore characterization test and its use in variability campaigns of comminution circuits. In Proceedings of the XXV International Mineral Processing Congress 2010, IMPC 2010, Brisbane, Australia, 6–10 September 2010.
22. Fonseca, E.D.; Vale, Santa Luzia, Minas Gerais, Brazil. Personal communication, 2017.
23. Barbosa, P.A.; Bergerman, M.G.; Fonseca, E. Evaluation of the LCPC Test for geometallurgical applications: Sossego mine case Study. In Proceedings of the IMPC 2020—XXX International Mineral Processing Congress, Cape Town, South Africa, 18–22 April 2021.
24. Monteiro, L.; Xavier, R.; Hitzman, M.; Juliani, C.; Souza Filho, C.; Carvalho, E.R. Mineral chemistry of ore and hydrothermal alteration at the Sossego iron oxide-copper-gold deposit, Carajás Mineral Province, Brazil. *Ore Geol. Rev.* **2008**, *34*, 317–336. [CrossRef]
25. Google Earth. Mina do Sossego. Available online: https://earth.google.com/web/search/mina+do+sossego/ (accessed on 7 August 2021).
26. Kwitko-Ribeiro, R. New sample preparation developments to minimize mineral segregation in process mineralogy. In Proceedings of the 10th International Congress for Applied Mineralogy (ICAM), Trondheim, Norway, 1–5 August 2011; Broekmans, M.A.T.M., Ed.; Springer: Berlin/Heidelberg, Germany, 2012; pp. 411–417. [CrossRef]
27. IMDEX Corporation. ioGAS™. Version 7.7. 2021. Available online: https://reflexnow.com/product/iogas/ (accessed on 7 August 2021).
28. Minitab®. Version 15.1. 2018. Available online: https://minitab.com/product/ (accessed on 10 May 2021).